JOURNAL OF MATERIALS SCIENCE 5 (1970) 240–247

A Study of Grinding Damage in Magnesium Oxide Single Crystals

B. G. KOEPKE, R. J. STOKES
Honeywell Corporate Research Center, Hopkins, Minnesota, USA

The sub-surface and surface damage produced by alumina and diamond grinding wheels has been studied as a function of material removal rate. Sub-surface damage is characterised in all cases by a discrete, dense layer of dislocations adjacent to the machined surface. The depth of the layer increases with material removal rate.

The nature of the surface damage depends on the mechanism of material removal. As long as the cutting points are unloaded and the residue can escape the material is removed in a brittle manner. This is always the case for the diamond wheel and occurs for low rates of material removal with the alumina wheel. When the cutting surface is loaded with residue, the tool-workpiece interface temperature becomes so high that the material is removed by plastic flow. The finished surface is burnished. Unfortunately as the burnished surface cools down thermal quenching produces a network of surface cracks.

1. Introduction

The nature and extent of damage introduced in ceramic oxides by abrasive machining operations is of considerable interest because it is well known that residual surface and sub-surface defects can seriously alter the physical and mechanical properties of a ceramic component. The exact nature of the damage, the manner by which it is generated and the depth to which it penetrates the surface, however, are not known. In fact, a recent review [1] of ceramic processing has pointed out that the grinding of ceramics is still an "art based on experience".

Throughout this paper two aspects of grinding damage will be discussed according to the following:

(i) Sub-surface damage, distinguished by the nature and depth of penetration of lattice defects introduced by the grinding operation.

(ii) Surface damage, distinguished by the dimensions and nature of cracks or flaws left in the machined surface.

The relative extent of sub-surface and surface damage depends on the nature of the material. Abrasion of completely brittle materials such as germanium [2, 3], silicon [3, 4], and sapphire [5] generally leads to a greater density of surface damage (non-crystallographic cracks) than sub-surface damage. Only a few isolated dislocations are generated at the extreme tips of the surface cracks. Semi-brittle materials on the other hand show profuse sub-surface damage following abrasion or wear [6–8]. Broad bands of slip are generated under the abrading particles, their extent depending on the temperature and yield stress of the workpiece. There is, in addition, some cracking.

This paper describes the results of an investigation of damage resulting from surface grinding operations performed on magnesium oxide crystals. Magnesium oxide falls in the semi-brittle category [9]. It is an ideal material for such a study because of the {100} cleavage geometry, the limited plasticity, and the ability to reveal clearly sub-surface and surface damage by etching. Rough and semi-finish grinding operations were chosen for study because it was felt that the severe damage introduced during the early stages of a finishing operation perpetuate and constitute the major source of flaws in the finished part.

2. Experimental Procedure

The specimens consisted of magnesium oxide crystals cleaved into rectangular slabs. Prior to grinding, all crystals were annealed 1 h at 1200° C in air. This treatment is sufficient to pin all existing dislocations and place the material in a

uniform starting condition with respect to mechanical behaviour [10]. Grinding was performed on (001) cleavage faces with the crystal moving in the [$\bar{1}$00] direction as shown in fig. 1a. (All directions and surfaces quoted in this paper refer to fig. 1a.) This geometry is convenient because other {100} faces normal to the ground surface may be exposed by cleavage and because the (101) and (10$\bar{1}$) slip planes are at 45° and therefore most favourably oriented for shear.

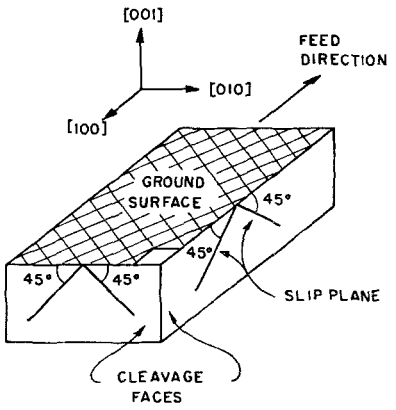

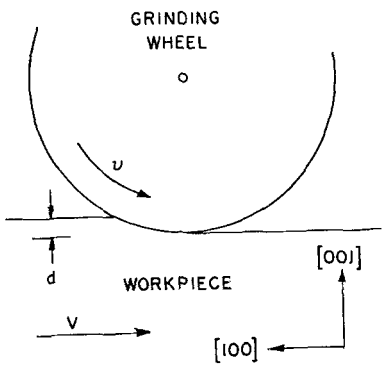

Figure 1 Grinding and crystal geometry used in surface grinding experiments: (a) crystal geometry; (b) grinding geometry.

Grinding was carried out using two wheels having significantly different structures. A 46 grit, vitrified bond alumina wheel containing many voids in its surface (see fig. 2a) had a relatively open structure, whereas a 100 grit, resinoid bond diamond wheel containing abrasive particles protruding from a continuous matrix (fig. 2b) had a closed structure.

All crystals were ground with the cutting face

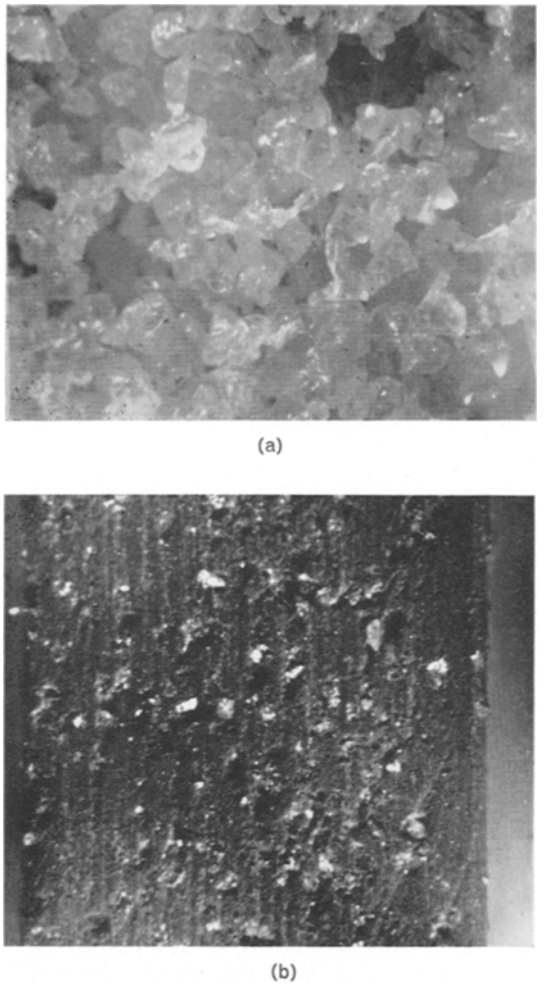

Figure 2 Photomicrographs of the cutting faces of the grinding wheels: (a) 46 grit, vitrified bond alumina wheel; (b) 100 grit, resinoid bond diamond wheel (× 33).

of the wheel moving in the same direction as the workpiece as shown in fig. 1b (climb grinding). Most attempts to machine in the opposite direction resulted in shattering of the specimens. Crystals were ground both wet and dry. The coolant used for wet grinding was water containing water-soluble oil in the ratio 80:1. The grinding parameters of interest were, workpiece feed rate V and depth of cut d (see fig. 1b). Feed rates varied from 0.042 to 4.2 cm sec^{-1} (1 to 100 in. min^{-1}) and depths of cut ranged from 12.7 to 508 μm (0.0005 to 0.020 in.).

Following the machining operation the specimens were examined optically both before and after etching to reveal dislocation configurations.

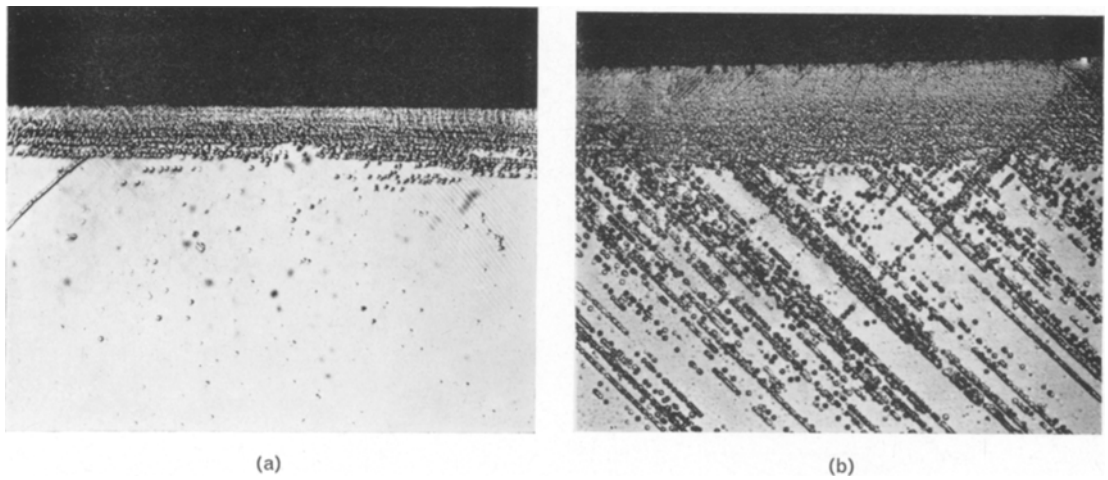

Figure 3 Etched (010) cleavage faces of crystals ground wet in one pass to varying depths of cut (d) with the alumina wheel (feed rate (V) = 0.055 cm sec^{-1}). (a) d = 25.4 μm, $D \simeq$ 47 μm; (b) d = 508 μm, $D \simeq$ 87 μm (× 180).

3. Observations of Sub-surface Damage

A discrete, severely deformed layer was found under the ground surface of every machined magnesium oxide crystal. The layer is clearly delineated by a dense band of dislocation etch-pits on (100) and (010) cleavage faces as shown below. The nature and dimension of this damage layer has been studied as a function of the grinding parameters using the alumina and diamond wheels.

3.1. Alumina Grinding Wheel

Photomicrographs showing the damage layers on (010) cleavage surfaces of magnesium oxide crystals ground to various depths of cut at a constant feed rate of 0.055 cm sec^{-1} are presented in fig. 3. The depth of the deformed layers clearly increases with the depth of cut. When the depth of cut is small (i.e. less than 127 μm) the damage layer is well-defined and uniform in thickness over the whole specimen as shown in fig. 3a. When the depth of cut is 254 μm and greater there is a distinct change in appearance of the etched layer as shown in fig. 3b. Slip bands on (101) and (10$\bar{1}$) planes penetrate well beneath the discrete layer itself. Note that although the rate of material removal (defined as the product of d and V) in fig. 3b is twenty times that in fig. 3a, the depth of damage, D is only about three times as great. Extremely severe machining operations using the alumina wheel can cause gross plastic deformation of the whole sample. In this case slip-bands extend almost completely through the crystal.

Since the depths of the damage layer at low rates of material removal were constant over the surface of any given specimen, the average depth, D, could be taken as a parameter to indicate the response of the material to the conditions generated at the tool-workpiece interface during grinding. Figs. 4 and 5 are plots of D against the rate of material removal, dV, for the 46 grit alumina wheel.

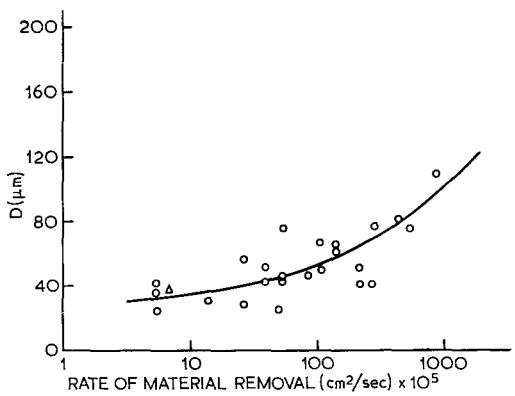

Figure 4 Depth of damage as a function of rate of material removal for crystals ground wet with a 46 grit alumina wheel. ○, single pass cuts; △, multi-pass 12 μm cuts.

A number of interesting points arise in connection with these figures. First, comparison of figs. 4 and 5 shows that crystals ground dry exhibited deeper damage than crystals ground in flowing coolant at all but the lowest material removal rates. Secondly, the depth of the damage

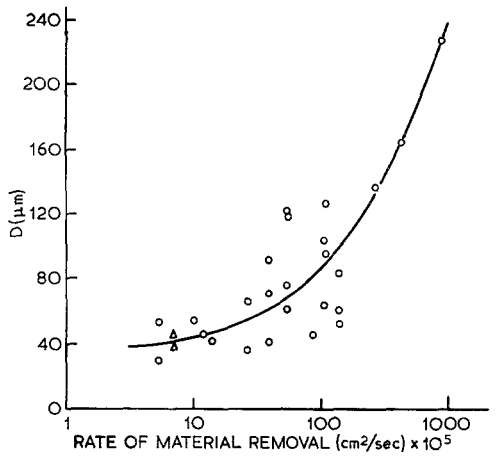

Figure 5 Depth of damage as a function of rate of material removal for crystals ground dry with the alumina wheel. ○, single pass cuts; △, multi-pass 12 μm cuts.

layer after multiple cuts at a given material removal rate is the same as if only a single pass had been made at the same rate, i.e. the damage is not cumulative. Thirdly, there is a lower limit to the depth of damage which by extrapolation in figs. 4 and 5 appears to be about 30 μm. Thus a 12.7 μm (0.0005 in.) cut generates a damage layer approximately three times its depth, whereas a 50 μm cut generates a damage layer less than its depth at slow feed rates. This should be contrasted with the observations of Marshall and Shaw [11] who noted that the depth of the deformed layer in annealed SAE52100 steel was only about one-half the depth of cut for 12.7 μm cuts.

3.2. Diamond Grinding Wheel

Observations of the etch-pitted damage layers in crystals ground with a 100 grit diamond wheel showed them to be significantly different from those ground with a 46 grit alumina wheel. The sub-surface deformed layer was not as uniform and well-defined even after light grinding. For example, fig. 6 shows the dislocation distribution on the two cleavage planes normal to the ground surface for a specimen machined with a 25.4 μm cut at 0.042 cm sec^{-1} (this should be compared with fig. 3a for the alumina wheel). There is evidence of a greater penetration of slip on the {110} planes at 45° to the ground surface. For instance, screw-dislocations on (011) or (0$\bar{1}$1) planes are visible as bands of etch-pits lying distinctly below and parallel to the ground surface in fig. 6a. Edge-dislocations on the same slip-planes are in rows of etch-pits at 45° to the ground surface in fig. 6b. It is also interesting to note that the surfaces exposed by cleavage contain dark regions as indicated by the arrow in fig. 6a. These originate from the interaction of the fracture fronts with this heavy {110} slip during cleavage.

The depth of damage in crystals ground with the 100 grit diamond wheel is plotted in fig. 7 as a function of the rate of material removal. Included on the plot are data from specimens ground with a single pass and specimens ground to 50 μm using multiple 12.7 μm cuts. Within the

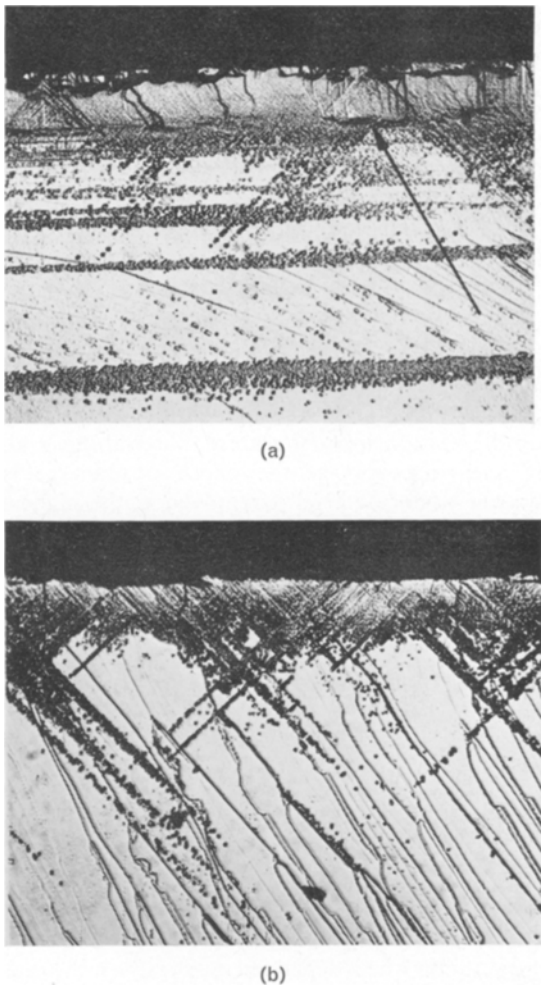

Figure 6 Etched {100} cleavage faces of a crystal ground wet with the diamond wheel (d = 25.4 μm, V = 0.042 cm sec^{-1} $D \simeq$ 47 μm): (a) (010) cleavage face parallel to grinding direction; (b) (100) cleavage face normal to grinding directions (× 160).

reproducibility and accuracy of the measurement, all results tended to follow a common curve. The scatter in D is to be expected from the cross-sectional view of the ground surface shown in fig. 6b. This scatter did not occur in most of the alumina ground samples presumably because of the lower density of slip on (0 1 1) and (0 $\bar{1}$ 1) planes.

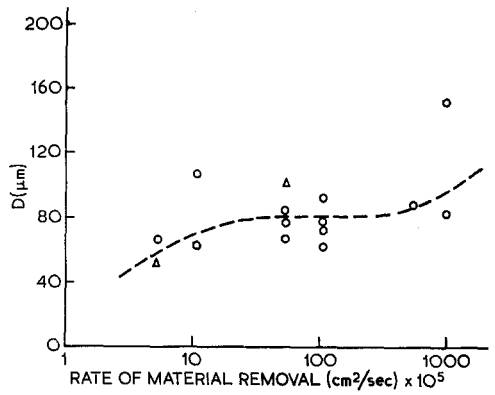

Figure 7 Depth of damage as a function of rate of material removal for crystals ground wet with the diamond wheel. ○, single pass cuts; △, multi-pass 12 μm cuts.

Referring to fig. 7, it is concluded that the depth of damage resulting from grinding with the 100 grit diamond wheel does not show any simple relationship to the rate of material removal. It does appear that the depth of damage is greater when material is removed at the highest rate.

4. Observations of Surface Topography

The surfaces produced by the respective grinding operations were examined optically and, using replicas, in the electron microscope. In some instances the surface features were enhanced by the etch used to delineate dislocations as described in the previous section. Again, differences were observed between surfaces produced by the alumina and diamond grinding wheels and they will be described separately.

4.1. Alumina Grinding Wheel

The surface topography of crystals ground with the alumina wheel depended distinctly on the rate of material removal. Grinding at low rates of material removal (i.e. corresponding to the extreme left side of figs. 7 and 5) produced irregular surfaces containing cleavage facets.

At higher rates of material removal with and without coolant the amount of cleavage decreased and the ground surfaces became quite smooth and burnished. Most significant was the appearance of regular arrays of fine cracks on the ground surfaces. These cracks lay in the plane normal to the ground surface and were generally oriented normal to the grinding direction. Observation of the fine surface cracks could be enhanced by etching as shown in fig. 8. The striking regularity of the surface cracks is also evident in this figure. In general it was observed that their number and extent increased with the rate of material removal. Note that the irregular patches of cleavage on the ground surface in fig. 8 are regions where material has been pulled out during machining. The "pull out" is clearly associated with the surface cracking.

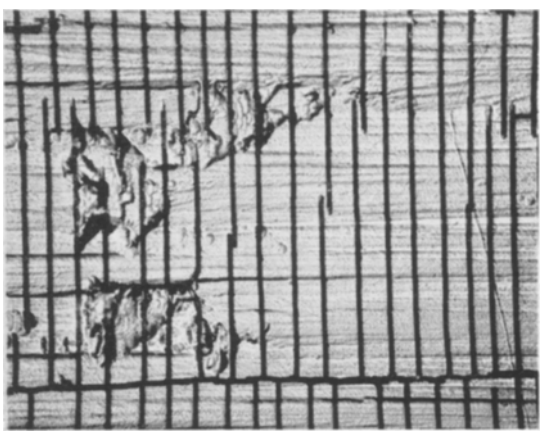

Figure 8 Etched {100} surface of a magnesium oxide crystal ground dry with the alumina wheel at a high rate of material removal ($d = 254$ μm, $V = 0.34$ cm sec^{-1}) ($\times$ 333).

4.2. Diamond Grinding Wheel

Surfaces ground with the diamond wheel at all rates of material removal were quite rough. In every case, the mechanism of removal involved brittle cleavage fracture. An example is shown in fig. 9. The white areas on the micrograph are cleavage facets parallel to the ground surface. The amount of cleavage fracture apparent on surfaces ground with the diamond wheel was found to increase with the rate of material removal. At no time did a surface ground with the diamond wheel show signs of burnishing.

5. Discussion of Results

In our opinion the most significant observations in this work relevant to understanding the tool-

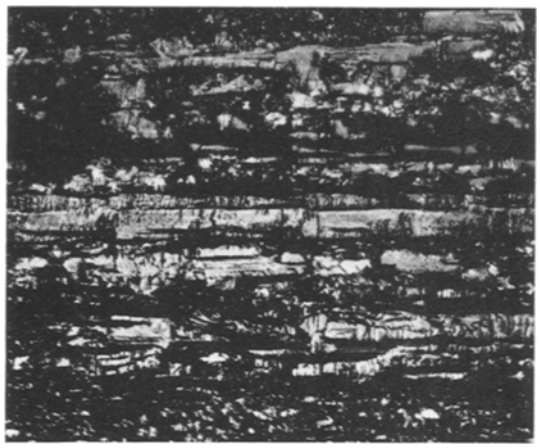

Figure 9 As-ground surface of a crystal ground wet with the diamond wheel at a medium rate of material removal ($d = 12.7$ μm, $V = 0.42$ cm sec^{-1}) ($\times$ 160).

workpiece interactions during ceramic machining are those which show a distinction in surface topography between crystals machined with alumina and diamond wheels. We believe that these differences primarily reflect different states of surface plasticity resulting from the grinding temperatures reached under the respective wheels.

In the case of the diamond wheel, the configuration of the cutting points on the surface of the wheel and the closed structure of the wheel itself (fig. 2b) result in material being gouged out by the individual diamond particles. The material is removed very efficiently by cleavage fracture (fig. 9) at all rates of material removal. Under these conditions there is little dissipation of energy in the form of plastic work during chip-formation and the grinding temperature at the crystal surface is not raised drastically.

In the case of the alumina wheel there is a difference between low and high rates of material removal. At low rates of material removal, the cutting points on the wheel remove and expel material from the machined surface in an efficient manner and the mechanism of material removal is again by brittle cleavage fracture. At high rates of material removal however debris is not expelled efficiently and the voids in the open structure of the wheel surface (fig. 2a) load up. (Note that in climb-grinding debris generated at the lead end of the cut must pass between the tool and workpiece.) Fresh cutting surfaces on the wheel are thus prevented from impacting the workpiece and the material must be removed by plastic flow or the workpiece will shatter. The plastic deformation involved in chip-formation generates heat causing an increase in the workpiece surface temperature. The plasticity of magnesium oxide, being strongly dependent on temperature [12], increases with the grinding temperature thereby further enhancing the workpiece plasticity and causing even more heating.

Under high strain rate conditions, the temperature must exceed 1500° C before the failure mode changes from the familiar brittle cleavage to ductile fracture [13]. Presumably then, temperatures in excess of 1500° C are being generated in the vicinity of the grinding wheel-workpiece interface. Temperatures of this magnitude have in fact been detected under a 46 grit alumina wheel on a high speed steel workpiece by Shaw and co-workers [14].

The burnished surface observed on {100} magnesium oxide crystals ground at high rates of material removal by an alumina wheel (fig. 8) is considered to be generated by high temperature plastic flow. An indication of the extent of plasticity was obtained by examination of the chips expelled during the machining operation using transmission electron microscopy. Electron transmission micrographs and diffraction patterns indicated complete recrystallisation of the chips, a phenomenon known to accompany very high temperature deformation [15].

The high surface temperatures generated during high rates of material removal with the alumina wheel also account for the regularly spaced surface cracks (fig. 8). These are considered to be initiated by the tensile stresses set up when the surface is quenched following passage of the wheel. To a first approximation the stress is given by

$$\sigma = E\alpha\Delta T$$

where E is Young's modulus, α is the coefficient of thermal expansion, and ΔT is the change in surface temperature during cooling. The fracture stress, σ_f, can be taken to be that given by the Griffith equation, namely

$$\sigma_f = \left[\frac{E\gamma_s}{C}\right]^{\frac{1}{2}},$$

where γ_s is the fracture surface energy and C is the flaw dimension. It is reasonable to approximate C to one-half the grit depth of cut. Backer *et al* [16], found the grit depth of cut to be 1.5 μm for steels ground with a 46 grit alumina wheel. Taking E to be 2.10×10^{12} dyne cm^{-2} [17], α to be 13.4×10^{-6} °C^{-1} [18] and γ_s to be

1150 erg cm^{-2} [19], it is found that cracking is to be expected when $\Delta T > 290°$ C. The cracks would not be expected to run very deep because of the extremely steep temperature gradients existing at the wheel-workpiece interface. This has been found to be the case as can be seen for instance in fig. 3 when the ground surface is cross-sectioned.

In addition to the steep temperature gradient just discussed, a steep stress gradient also exists at the surface of the crystals during grinding. In order to account for the observations it is suggested that grinding stresses arise in two ways; first, there are local stresses generated in the surface due to the impact of the individual cutting points, and second there are longer range stresses associated with the simple physical act of pushing the grinding wheel through the workpiece. We propose that the first stress field accounts for the discrete layers illustrated in fig. 3, whereas the second, longer range, stress field accounts for the bulk deformation illustrated in fig. 3b.

The presence of the plastically deformed layer adjacent to the ground surface of a magnesium oxide crystal is not surprising. Stokes *et al* [20] have shown that crystals of magnesium oxide may undergo large amounts of plastic deformation at room temperature providing dislocation sources are present initially (e.g. from surface indentations). The very nature of the grinding process causes the continual introduction of a high density of fresh dislocations due to the impact of each abrasive point of the wheel surface with the crystal workpiece. The high density of surface sources assures dense homogeneous slip under the action of the local stresses and accounts for the absence of any sub-surface cracking which might otherwise occur if slip were random and heterogeneous [20].

The relatively discrete nature of the layer in fig. 3 suggests that its depth D might possibly be defined by the intersection of active slip planes existing either under the contact area of the wheel as shown in fig. 10a or under adjacent cutting points on the wheel as illustrated in 10b. Depths of damage estimated by both of these models, however, are much higher than the values shown in figs. 4, 5 and 7 and it must be concluded that, although the slip geometry in magnesium oxide crystals is simple, geometrical arguments cannot be used to predict the observed values of D.

Rather, we consider the discreteness of the sub-surface deformed layer to reflect the steepness of the local stress and temperature gradients. The layer extends to the depth at which the shear stresses equal the yield strength of the crystal.

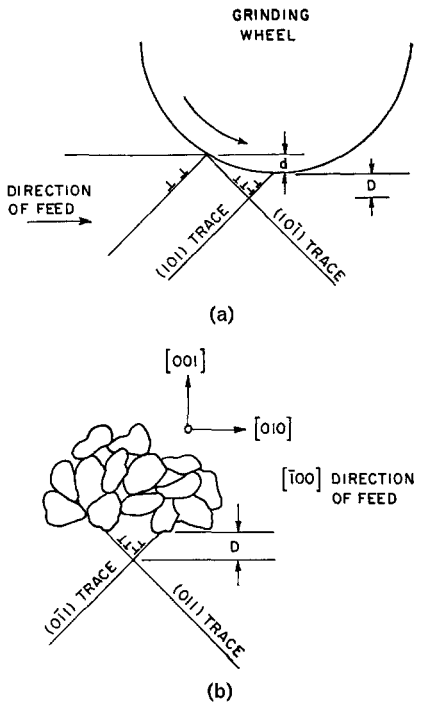

Figure 10 Schematics showing how the depth of the plastically deformed layer, D, might be related to the intersection of active slip bands: (a) Slip activated under the contact area of the wheel; (b) slip activated by adjacent cutting points on the wheel surface.

The onset of bulk deformation at high rates of material removal illustrated in fig. 3b corresponds to the situation where the grinding wheel cannot remove material fast enough from the surface. The crystal is then essentially being forced through the machine between the grinding wheel and the grinding table. Obviously, if the material cannot undergo bulk deformation extremely high reaction stresses will be generated causing rupture of either the specimen or the wheel.

In summary, the differences observed in the grinding damage introduced in magnesium oxide crystals by alumina and diamond grinding wheels at various rates of material removal are a direct consequence of the plasticity of the material. In crystals ground with the alumina wheel at moderate to high rates of material removal high temperature plasticity is involved in chip-formation and surface-burnishing. On the other hand, low temperature plasticity accounts for the generation of the discrete, highly de-

formed layer underneath surfaces ground with both the alumina and diamond wheels and results from the continual introduction of fresh dislocations during impact of the cutting points on the wheels with the workpiece. The bulk deformation of crystals (as denoted by discrete slip-bands penetrating beneath the surface layer) ground at high rates of material removal also occurs at ordinary temperatures. We conclude that the machinability of a ceramic is dependent on its fundamental plasticity.

If the facility for low temperature plastic deformation is removed then first, bulk deformation becomes impossible and the specimen shatters at high rates of material removal and second, the local stresses generated at the surface cannot be relieved by plastic flow but must be relieved by cracking instead. If the facility for high temperature plastic deformation is removed, then machining cannot occur by plastic flow and burnishing will not be observed. Attempts to machine completely brittle specimens at intermediate to high rates of material removal will only result in shattering. In such an instance the only mechanism for ceramic machining is the one observed here at low rates of material removal, involving brittle or cleavage fracture and efficient expulsion of the chips.

The consequences of changes in material plasticity on the machinability and surface finish of a variety of ceramics is continuing in our laboratory.

Acknowledgement

The support of this investigation by the Office of Naval Research under Contract No. N0014-69C-0123 is gratefully acknowledged. The authors are indebted to Dr C. H. Li for his continued interest and to D. Woodward for his able experimental assistance.

References

1. "Ceramic Processing", Publication 1576 (National Academy of Sciences, Washington, DC, 1968) p. 145.
2. L. N. PUGH and L. E. SAMUELS, *Phil. Mag.* **8** (1963) 301.
3. R. L. MEEK and M. C. HUFFSTUTLER JR, *J. Electrochem. Soc.* **116** (1969) 893.
4. R. STICKLER and G. R. BOOKER, *Phil. Mag.* **8** (1963) 859.
5. R. P. STEIJN, *J. Appl. Phys.* **32** (1961) 1951.
6. *Idem, ibid* **34** (1963) 419.
7. R. P. BOWDEN and C. A. BROOKES, *Proc. Roy. Soc.* **A295** (1966) 244.
8. C. A. BROOKES and J. B. O'NEILL, "Anisotropy in Single-Crystal Refractory Compounds", edited by F. W. Vahldick and S. A. Mersol (Plenum Press, New York, 1968) p. 291.
9. R. J. STOKES, *Fund. Phen. Matl. Sci.* **4** (1967) 151.
10. *Idem, J. Amer. Ceram. Soc.* **48** (1965) 60.
11. E. R. MARSHALL and M. C. SHAW, *Trans. ASME* **74** (1952) 51.
12. R. B. DAY and R. J. STOKES, *J. Amer. Ceram. Soc.* **47** (1964) 493.
13. T. L. JOHNSTON, R. J. STOKES, and C. H. LI, *Phil. Mag.* **4** (1959) 1316.
14. J. E. MAYER and M. C. SHAW, *Lubric. Eng.* **13** (1957) 21.
15. J. E. BAILEY, "Electron Microscopy and Strength of Crystals", edited by G. Thomas and J. Washburn (Wiley, New York, 1963) p. 535.
16. W. R. BACKER, E. R. MARSHALL, and M. C. SHAW, *Trans. ASME* **74** (1952) 61.
17. W. D. KINGERY, "Introduction to Ceramics" (Wiley, New York, 1960) p. 599.
18. *Idem, ibid*, p. 473.
19. A. R. C. WESTWOOD and D. L. GOLDHEIM, *J. Appl. Phys.* **34** (1963) 3335.
20. R. J. STOKES, T. L. JOHNSTON and C. H. LI, *Phil. Mag.* **6** (1961) 9.

Received 11 November and accepted 30 December 1969